13th World Conference on Earthquake Engineering
Vancouver, B.C., Canada
August 1-6, 2004
Paper No. 346

A SIMPLE PROPOSAL FOR SEISMIC DEMAND EVALUATION OF STEEL FRAMED STRUCTURES BASED ON SIMPLIFIED SAFETY DOMAIN

Takumi ITO[1] and Kenichi OHI[2]

SUMMARY

To simplify the non-linear dynamic design procedure on steel framed structures to seismic actions, a new design-friendly reduced analysis is proposed as a vibration-mode failure-mode integrated analysis. The present method is based on two kinds of simplified plastic surface model: one modeling is a yield polyhedron model with reduced number of failure modes, and another much simpler model is a yield hyper-ellipsoidal model. The validity of the simplified analyses proposed is checked by comparison with a pseudo-dynamic response test on a 2-story steel frame specimen and a detailed analysis on a 9-story 3-bay frame model.

INTRODUCTION

The emphasis in seismic resistance design is shifting from “strength” to “performance” following the demand and collapse of numerous structures during recent earthquake. Gradually, performance based designs are becoming a part of code provisions with publication of FEMA-273 [1] in USA and Enforcement Order and Regulation after Building Standard Law of Japan was revised in 1998 [2]. At the same time, it may be fair to say that simple and efficient methods for capturing the essential and important features affecting the performance have not been adequately developed. The objective of this paper is to develop a design friendly method for performance evaluation of ductile steel moment-resisting frames, which are used as the primary lateral load resisting systems in many middle-rise buildings. Proposed research focuses on the simplifications of non-linear dynamic design procedures (NDP). This study intends to benefit the design engineer by bringing NDP, which is usually considered complicated and costly, within the reach of a structural engineer, who is familiar with linear dynamic analysis.

This paper presents a non-linear dynamic procedure with partial-mode response analysis with simplified plastic failure surface models. A safety domain about plastic collapse of an elastic-perfectly plastic frame is approximated by a yield polyhedron with a reduced number of failure modes. To reduce the number of failure modes, a preliminary analysis based on first-order second-moment (FOSM) reliability method is proposed by Khandelwal [3]. This method requires, however, an exhaustive procedure to enumerate the

[1] Postdoctoral Research Fellow, IIS, the Univ. of Tokyo, JAPAN. Email: takumi@iis.u-tokyo.ac.jp
[2] Professor, Kobe University, JAPAN. Email: ken_ichi_ohi@hotmail.com

whole failure mechanisms, and the failure surface becomes a convex polyhedron made of a lot of hyper surfaces even after they are reduced. Sometimes it happens to encounter the problem of dealing with extreme points during the renewal procedure of restoring force. To avoid them, an alternative method is proposed in this paper. The plastic failure surface is approximated by a hyper-ellipsoidal model, which has no extreme point and provides a much easier procedure to trace the inelastic global behavior than the yield polyhedron model. Additionally, the method proposed does not require the enumeration of enormous failure mechanisms to arrange the hyper-ellipsoidal yield surface.

And then, the validity of the proposed response analysis here is checked by comparison with a detailed computer analysis on a 9-story 3-bay steel moment-resisting frame as well as a pseudo-dynamic response test on a 2-story 1-bay steel frame specimen.

PARTIAL MODE RESPONSE ANALYSIS IN MODAL SPACE

The equation of motion for a multi-degree-of-freedom system with viscous damping and hysteretic inelastic restoring force under seismic excitation is represented as:

$$[M]\cdot\{\ddot{x}\}+[C]\cdot\{\dot{x}\}+\{f\}=-[M]\cdot\{1\}\,\ddot{g}_0 \tag{1}$$

where $[M]$ is mass matrix, $[C]$ is damping matrix, $\{\ddot{x}\}$ are $\{\dot{x}\}$ acceleration vector and velocity vector relative to the ground, respectively, $\{f\}$ is restoring force vector including plastic resistance of a frame, and $\ddot{g}_0$ is the ground acceleration.

Here we define the transformation of displacement relative to the ground $\{x\}$ and restoring force into modal coordinates as:

Transformation of displacement: $\{x\}=[\Phi]\cdot\{q\}$ (2)

Transformation of restoring force: $\{f\}=\left[\Phi^T\right]^{-1}\cdot\{r\}=[\Psi]\cdot\{r\}$ (3)

where $\{q\}$ is modal displacement vector, $\{r\}$ is modal restoring force vector, $[\Phi]$ is modal participation matrix based on classical normal modes for a linear-elastic frame system $=[{}_1\beta\{{}_1u\},\ {}_2\beta\{{}_2u\},\cdots,\ {}_n\beta\{{}_nu\}]$, n is the number of vibration modes, and $\{{}_j\psi\}$ is the j-th base vector for force given as a column vector of $[\Psi]=\left[\Phi^T\right]^{-1}$.

By this transformation, the equation of motion on the modal space is given by:

$${}_j\ddot{q}+2\ {}_jh\ {}_j\omega\ {}_j\dot{q}+{}^jr\Big/{}_jM^*=-\ddot{g}_0 \tag{4}$$

where ${}_jh$ is the j-th modal damping constant, ${}_j\omega$ is the j-th natural circular frequency, and ${}_jM^*$ is the j-th effective mass.

It should be noted that the modal coordinate used herein is just regarded as one of possible generalized coordinates, and it is not expected in the procedure to turn a stiffness matrix diagonal as done in a linea-elastic modal analysis, because any stiffness matrix does not appear explicitly in Eqs.(1) and (4). Inelastic restoring force $\{f\}$ and then inelastic modal restoring force $\{r\}$ can be traced after any kind of hysteresis rule or algorithm (or sometimes measured from a loading test).

The modal displacement increment can be calculated based on an explicit numerical integration (central finite difference) from the j-th modal component of restoring force:

$$\Delta q_j^{\,k\to k+1} = \frac{\left(1-{}_j h\ {}_j\omega\,\Delta t\right)\Delta q_j^{\,k-1\to k} - \Delta t^2\left({}_j r \,/\, {}_j M^* + \ddot{g}_0\right)}{\left(1+{}_j h\ {}_j\omega\,\Delta t\right)}\ ,\ j=1,2,\cdots,n'\le n \qquad (5)$$

where $\Delta q_j^{\,k\to k+1} = {}_j q^{(k+1)} - {}_j q^{(k)}$, n' is the number of partial vibration modes.

So far as all the vibration modes are considered, this analysis is strictly equivalent to the inelastic response analysis performed in the ordinary coordinate system. Furthermore, it is feasible to limit the vibration modes considered in the analysis to only a small number of relevant vibration modes (usually several lower-frequency modes are chosen). Such a technique of partial mode analysis is adopted in the following response analyses.

SIMPLIFIED PLASTIC FAILURE SURFACE MODELS

In this paper, the following two types of simplified plastic surface models are discussed. (1) One is a yield polyhedron model with reduced number of failure modes by the first-order second-moment reliability method (Khandelwal [3]), and (2) the other is a yield hyper-ellipsoidal model arranged to share some exact reference points on the yield surface obtained from pushover limit analysis. In this safety domain against plastic collapse, sequence of yielding before mechanism formation i.e. partial yielding is ignored (**Fig.1**).

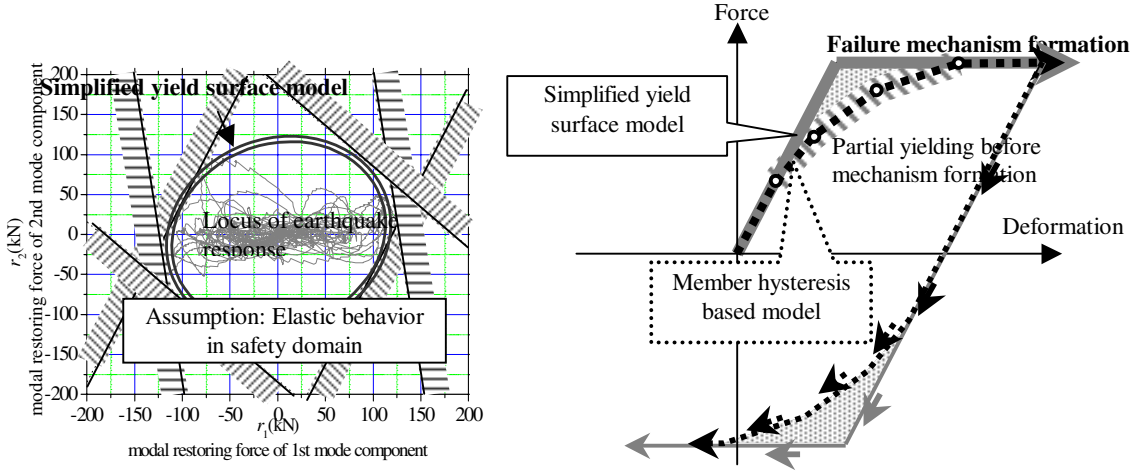

Fig.1 Skelton curves of member hysteresis based frames and simplified failure surface models

Reduced yield polyhedron model

A simple proposal to calculate global inelastic responses of MDOF steel moment-resisting frame was made by one of the authors [3], where a global yield surface model of a frame was arranged and simplified based on the limit analysis and the first-order second-moment reliability method. First, a procedure was proposed for 'vibration mode – failure mode' integrated analysis, wherein the restoring force characteristics are represented by a global convex yield polyhedron model, instead of a set of member-hysteresis based models usually adopted in the inelastic structural analysis. Then FOSM is extended to choose an appropriate number of failure modes to be considered in the analysis.

Equivalent-static seismic loading model

A simple equivalent-static seismic loading model for linear-elastic seismic load effect is adopted only in the preliminary analysis to choose important failure modes. As the ground motion varies randomly in time,

mean value or expected value of modal restoring forces is taken as zero, and the modal restoring forces of different vibration modes are assumed statistically independent (**Fig.2**). In a usual notation of $E(\ )$ for expected value:

$$E\left({}_j r\right)={}_j\bar{r}=0\,;\ E\left({}_i r\ \ {}_j r\right)=0\quad (i\neq j) \tag{6}$$

$$\sigma_{rj}=c\ \ {}_jM^{*}\ S_A\left({}_j h,{}_j\omega\right) \tag{7}$$

where σ_{rj} is standard deviation of the modal restoring force, c is a constant which is determined from the relationship between the standard deviation of modal restoring force at arbitrary points in time and its mean extreme as shown in **Fig.3** (Davenport [4]), and around one thirds for the value of c may be acceptable when an earthquake-like short duration are dealt with (Shibata [5]), $S_A({}_jh,\ {}_j\omega)$ is ordinate of acceleration response spectra, which depends on natural period and damping of j-th vibration mode.

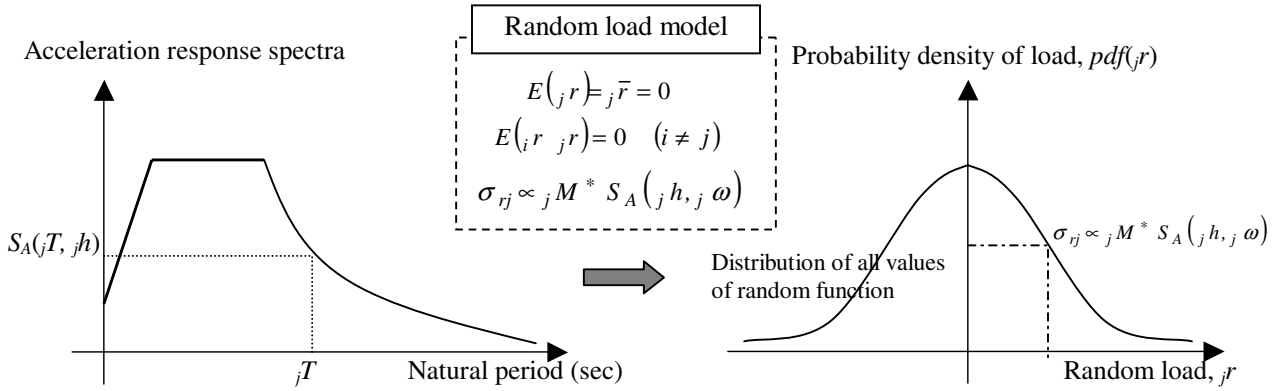

Fig.2 Random load model

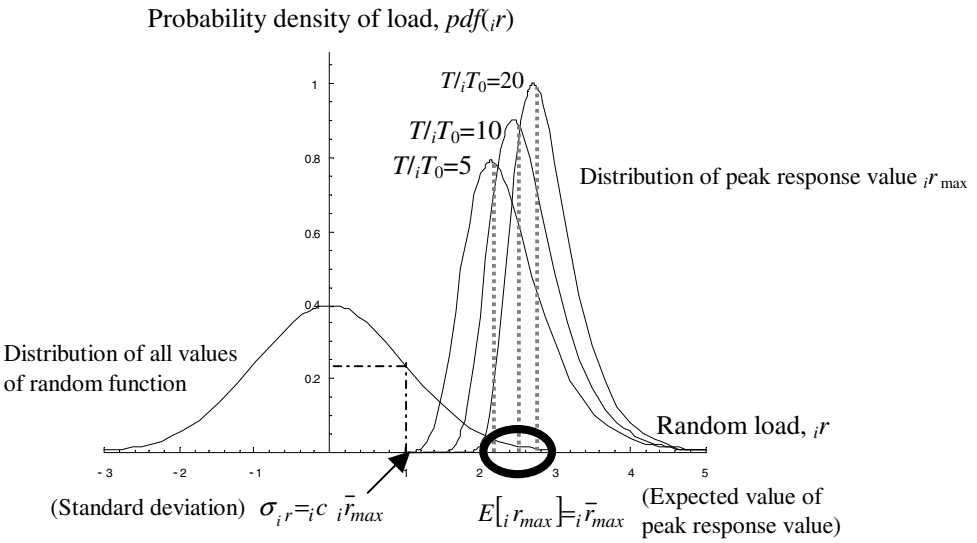

Fig.3 Probability density of random loading model and the peak response value

Reduction of failure modes

Stochastic limit analysis based on FOSM is applied herein for identification of more likely failure modes. It is assumed that the seismic action and the resistance are independent of each other. The performance or

limit state function, which is denoted by g and corresponding to each failure mechanism, can be written in terms of the energy dissipated by plastic portions and the work done by seismic action as:

$$g = \sum_{i=1}^{m} M_{P\,i}\left|\theta_{P\,i}\right| - \sum_{j=1}^{n} {}_{j}q_{P}\left|{}_{j}r\right| \tag{8}$$

where m is number of plastic portions (plastic hinges). The energy dissipated by plastic portions is represented by the sum of $M_{P\,i}\,|\theta_{P\,i}|$ ($i = 1, 2, \cdots, m$), where $M_{P\,i}$ is the basic variable of element moment capacity and $|\theta_{P\,i}|$ denotes the rotation of the corresponding plastic hinge. The work done by the seismic action is expressed in the modal coordinates and represented by the sum of ${}_{j}q_{P}\,|{}_{j}r|$ ($j = 1, 2, \cdots, n$), where ${}_{j}q_{P}$ is the j-th modal component of plastic deformation compatible with the before-mentioned plastic hinge rotations.

Mean value of g: $\mu_g = \sum_{i=1}^{m} \overline{M}_{P\,i}\left|\theta_{P\,i}\right| - \sum_{j=1}^{n} {}_{j}q_{P}\,{}_{j}\bar{r}$ (9)

Standard deviation of g: $\sigma_g = \sqrt{\sum_{i=1}^{m}\left(\sigma_{M_{P\,i}}\right)^2\left(\theta_{P\,i}\right)^2 + \sum_{j=1}^{n}\left({}_{j}q_{P}\right)^2\left(\sigma_{r\,j}\right)^2}$ (10)

where $\overline{M}_{P\,i}$, ${}_{j}\bar{r}$ are mean values and $\sigma_{M_{P\,i}}, \sigma_{r\,j}$ are standard deviation of resistance capacity and random load model, respectively.

As the mean values of seismic action is taken zero if we adopt the equivalent-static model in the previous section, the FOSM reliability index, denoted by β corresponding to the failure mechanism is given by:

$$\beta = \frac{\mu_g}{\sigma_g} = \frac{\sum_{i=1}^{m} \overline{M}_{P\,i}\left|\theta_{P\,i}\right|}{\sqrt{\sum_{j=1}^{n}\left({}_{j}q_{P}\right)^2\left(\sigma_{r\,j}\right)^2}} \tag{11}$$

A lower reliability index indicates higher probability of failure. In our view, failure mechanisms with probability less than about 10% of the most likely (β_{min}) failure mechanism can excluded from further analysis. Alternatively, failure mechanisms with $\beta \geq \beta_{min} + \Delta$ can be neglected. In case of a normal distribution and $\beta_{min} \geq 1.4$, Δ equal to unity would be adequate. In addition, the maximum number of failure mechanisms considered should preferably be limited to the number of vibration degrees of freedom, to avoid possibility of ill conditioning during dynamic analysis (**Fig.4**).

For structures with very large numbers of potential failure mechanisms, mutual correlation between the failure mechanisms should be considered, as many of them may be partially correlated. PNET (Ang [6]), which stands for probabilistic network evaluation technique, can be applied for such a situation. The correlation coefficient between the two failure modes, a and b, can be written as:

$$\rho_{ab} = \frac{E\left[\left(g_a - E(g_a)\right)\left(g_b - E(g_b)\right)\right]}{\sigma_{g\,a}\,\sigma_{g\,b}} \tag{12}$$

where these performance functions are determined by Eq.(8) with ${}_{j}q_{P}$, ${}_{j}a$ and ${}_{j}b$, corresponding to each mechanism shape.

If we ignore the uncertainty of moment capacities, they can be written as:

$$\rho_{ab} = \frac{\sum_{j=1}^{n} {}_j a \ {}_j b \, \sigma_{r\,j}}{\sqrt{\sum_{j=1}^{n} ({}_j a)^2 (\sigma_{r\,j})^2 \sum_{j=1}^{n} ({}_j b)^2 (\sigma_{r\,j})^2}} \tag{13}$$

Failure mechanisms with correlation coefficients more than a demarcating correlation are unified and represented by a single failure mechanism having lowest reliability index among them, as shown in **Fig.4**.

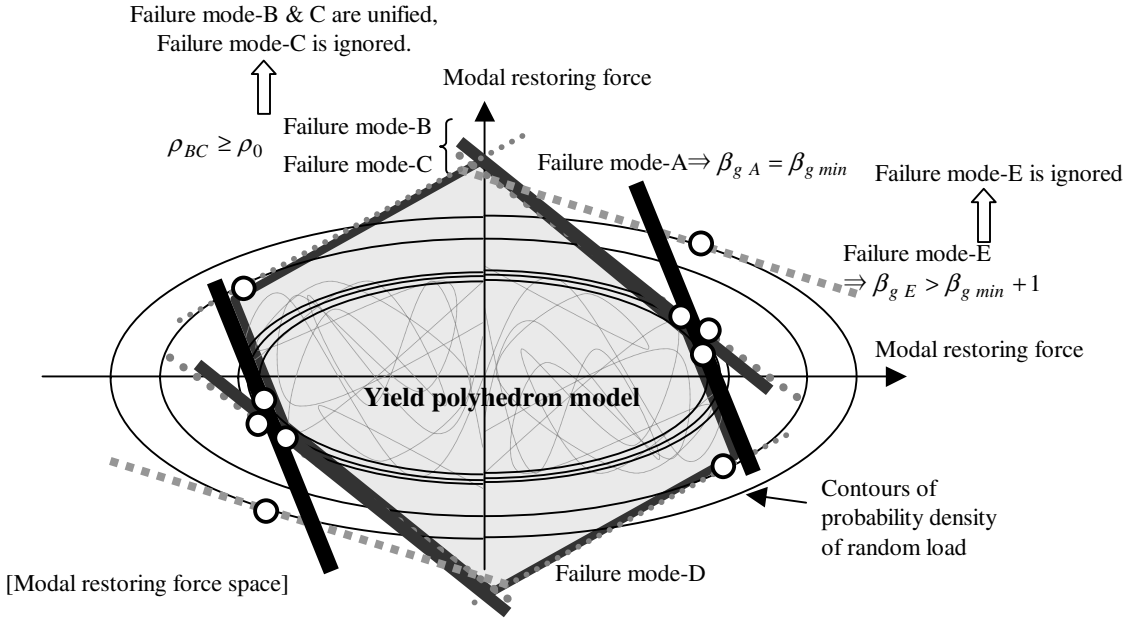

Fig.4 Reduction of failure modes based on first-order second-moment reliability method

Ellipsoidal yield surface model

Another much simpler approach is proposed by use of an ellipsoidal approximation of global safety domain against plastic collapse. From general view of exact safety domain, an ellipsoidal body can outline a convex figure of exact yield polyhedron. Such a hyper-ellipsoid in *n*'-dimensional force space can be determined so that it shares different reference points on the exact yield surface. Then pushover limit analysis on a frame under different load patterns is performed to obtain these reference points, and the safety domain is approximated by an *n*'-dimensional hyper-ellipsoidal body.

Pushover limit analysis to obtain reference points

As for the limit analysis of the frames by computer, the following problem is solved:

Maximize: λ

Subject to equilibrium equation: $\lambda \{P_0\} = [\quad Con. \quad] \cdot \{M\}$ (14)

and yield condition of members: $|M_i| \leq M_{P\,i}$

where λ is load factor, $\{P_0\}$ is load pattern vector, [*Con.*] is connectivity matrix, $\{M\}$ is element moment vector, $M_{P\,i}$ is element moment capacity of M_i.

It is convenient to represent the load pattern vector as a linear combination of modal load patterns corresponding to elastic seismic load effects as adopted in the previous section. In a general form, it is expressed by:

$$\lambda\{P_0\} = \lambda[\Psi]\cdot\{r\} = \lambda_1 r\{{}_1\psi\} + \lambda_2 r\{{}_2\psi\} + \cdots + \lambda_n r\{{}_n\psi\} \tag{15}$$

Load pattern used in pushover limit analysis

When each peak value of modal force component is given beforehand as shown in **Fig.5**, it is the most conservative condition to consider that each modal force reaches its peak value at the same time. In this assumption the locus of modal force may spread over a rectangular area as shown in **Fig.5**. In an alternative condition, when one component reaches its peak value, other modal forces may be assumed to remain their averages according to Turkstra's rule. This assumes that the locus of modal force exists within a diamond area as shown in **Fig.5**. These two conditions are extreme assumptions of modal force combination. Square Root of Sum of Square (SRSS) is another intermediate condition sometimes adopted, and it corresponds to an elliptical area. Thus, a few different assumptions are possible about the area in which the modal force point likely exists. In this paper, the following two kinds of load patterns are adopted to represent the locus of modal load effect: (1) A load pattern aiming at the sharpest corner of the diamond area (the most predominant mode pattern only), (2) combined load patterns aiming at corners around the most far side of the rectangular are (the most predominate mode pattern plus and minus other mode patterns). This selection includes $2n$'-1 different load patterns.

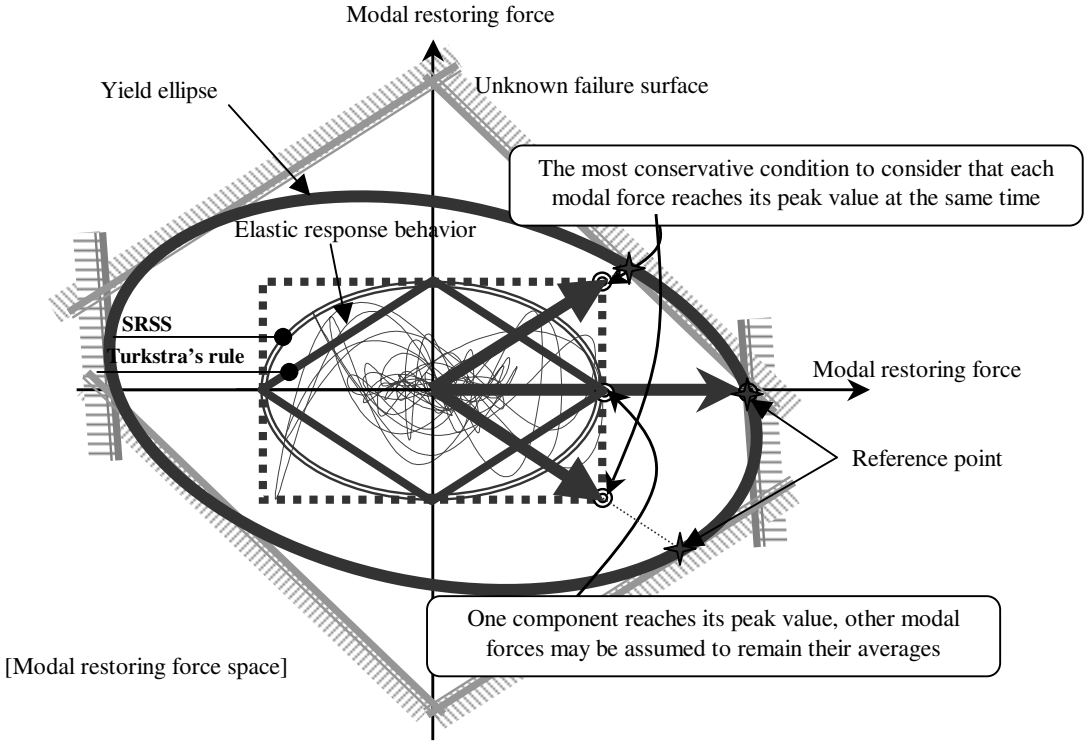

Fig.5 Load pattern used in pushover limit analysis

If we choose two dominant load patterns denoted by $\{{}_i\psi\}$ and $\{{}_j\psi\}$ instead of considering all the vibration modes, and if we consider the ratio of dominancy based on the magnitude of elastic seismic load effect, then a simplified load pattern may take the following form:

Load pattern 1: $\lambda\{P_0\} = \lambda_i r\{{}_i\psi\}$ (16)

Load pattern 2: $\lambda\{P_0\} = \lambda_{\ i}r\{{}_i\psi\} \pm \lambda\,\alpha_{ij}\ {}_jr\{{}_j\psi\}$ (17)

where $\alpha_{ij} = \dfrac{{}_jM^*\ S_A({}_jh,\ {}_j\omega)}{{}_iM^*\ S_A({}_ih,\ {}_i\omega)}$, $({}_iM^*\ S_A({}_ih,\ {}_i\omega) > {}_jM^*\ S_A({}_jh,\ {}_j\omega))$

Determination of hyper-ellipsoidal body

After the load is determined, the limit analysis of the structure is performed to obtain the reference points. These reference points are supposed to satisfy the following equation:

$$\{r^*\}_k^T \cdot [A] \cdot \{r^*\}_k = 1,\ k = 1, 2, \cdots, 2n'-1 \tag{18}$$

where [*A*] is a symmetrical matrix that controls the shape and the inclination of the *n*'-th dimensional hyper-ellipsoidal body. The number of indeterminate maximum but we assumed the following simplified form and reduce it to 2*n*'-1, and then they can be determined by solving the simultaneous equation (19).

$$[A] = \begin{bmatrix} a_1 & a_2 & \cdots & a_{n'} \\ a_2 & a_{n'+1} & 0 & 0 \\ \vdots & 0 & \ddots & 0 \\ a_{n'} & 0 & 0 & a_{2n'-1} \end{bmatrix} \tag{19}$$

EXAMPLE OF LOW-RISE STEEL MOMENT-RESISTING FRAME

Pseudo-dynamic response test is applied for low-rise steel moment-resisting frame to check the validity of the response analysis proposed in the previous sections.

Pseudo-dynamic response test of 2-story 1-bay steel moment-resisting frame specimen

Fig.6 illustrates the test specimen of 2-story 1-bay steel frame. A specimen consists of H-shaped column and beam (H-125 × 125 × 6.5 × 9, JIS SS400 grade steel) and mechanical properties of material are summarized in **Table 1**. The connections of beam and column fastened by high-strength pre-tensioned bolts with cover plates and splice plates are considered as rigid zone. All the H-shaped members are placed in a so unusual way to be bent about the weak axis. This arrangement prevents lateral and local buckling of members and out-of-plane instability of the specimen frame, and then only a single-plane frame can be loaded by two electro-hydraulic actuators.

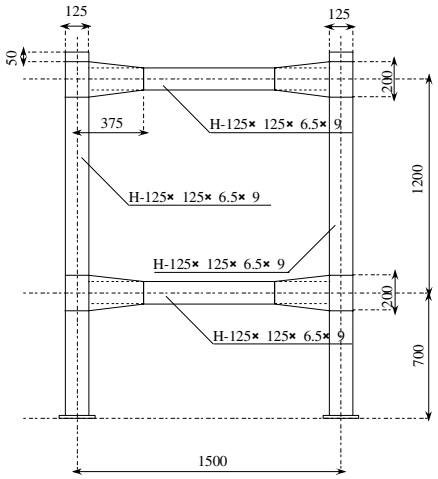

Fig.6 Test specimen of 2-story 1-bay steel moment-resisting frame

Table 1 Mechanical properties of material

Yield stress	Tensile strength	Elongation
348 N/mm^2	461 N/mm^2	21%

Sum of fictitious inertial mass of 2nd floor and roof of the frame is 20,000kg. As for the mass distribution, two ratios of the 2nd floor to roof are taken herein: one (or uniform mass), three (or three times larger mass at the 2nd floor). Of course the basic load modes depend on these mass ratios. Fictitious damping is 2.0% in 1st and 2nd modes, and the base shear coefficient of the structure is estimated 0.62, 0.79.

Table 2 Properties of pseudo-dynamic test and completely numerical response analysis

Mass distribution	M_1/M_2=1		M_1/M_2=3	
Mode	1st	2nd	1st	2nd
Natural period	0.27 sec	0.09 sec	0.21 sec	0.10 sec
Effective mass	14,700 kg	5,300 kg	13,700 kg	6,300 kg
Participation vector $\beta\{u\}$	0.29 1.17	0.71 -0.17	0.42 1.49	0.58 -0.49
Shear strength coefficient	0.62		0.79	

Pseudo-dynamic response tests were performed on the above-mentioned structure subjected to the ground acceleration record of El Centro 1940 NS and also an acceleration impulse. The peak ground acceleration of El Centro 1940 NS was scaled to 10m/sec^2, and the initial velocity induced by the impulse to the frame is set 0.7m/sec. Simulated time were 10sec for El Centro 1940 NS and 3sec for the impulse, respectively. And the time increment Δt was taken 0.005sec commonly for response calculation. **Fig.7 (a)** and **Fig.8 (a)** show the loci of modal restoring force during the pseudo-dynamic response tests.

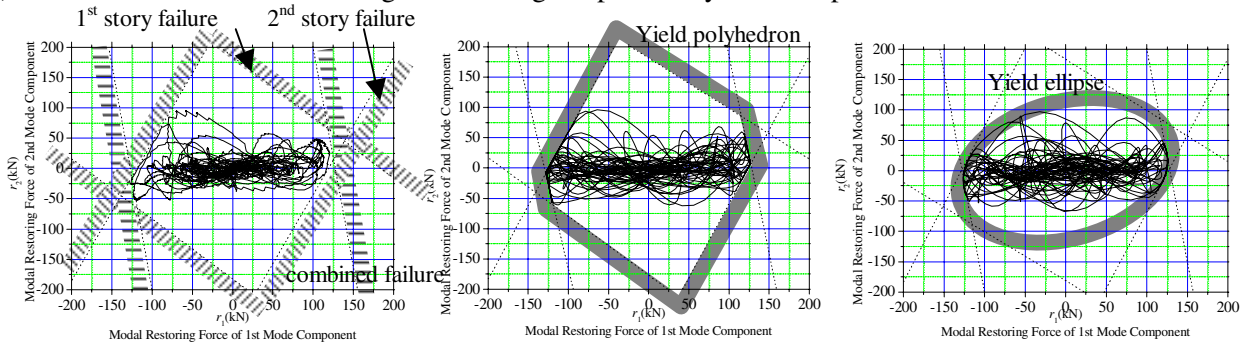

(a) Pseudo-dynamic response test (b) Yield Polyhedron (c) Yield ellipse

El Centro 1940 NS, (PGA: 1.0m/sec^2)

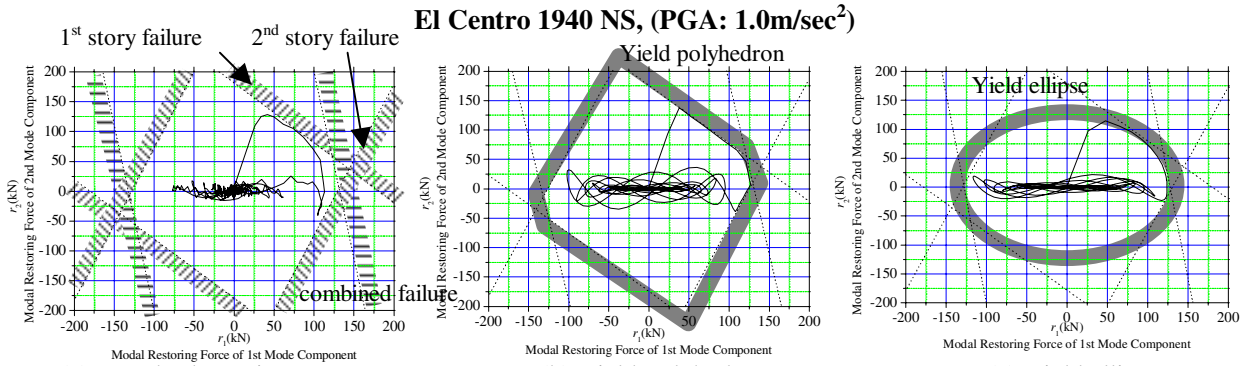

(a) Pseudo-dynamic response test (b) Yield Polyhedron (c) Yield ellipse

Acceleration impulse, (PGV: 0.7m/sec)

Fig.7 Loci of modal restoring force (mass distribution, M_1/M_2=1)

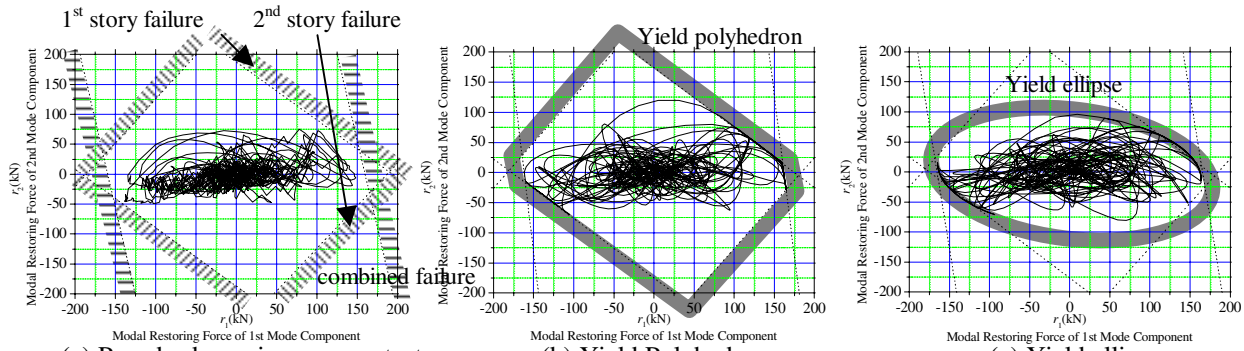

(a) Pseudo-dynamic response test (b) Yield Polyhedron (c) Yield ellipse

El Centro 1940 NS, (PGA: 1.0m/sec^2)

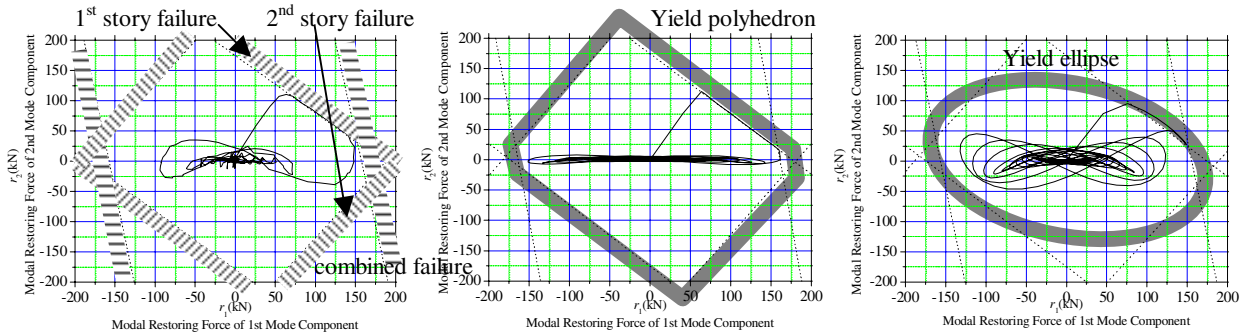

(a) Pseudo-dynamic response test (b) Yield Polyhedron (c) Yield ellipse

Acceleration impulse, (PGV: 0.7m/sec)

Fig.8 Loci of modal restoring force (mass distribution, M_1/M_2=3)

Response analysis based on an elliptic plastic failure surface model

Fig.9 shows the elliptic yield surface model of 2-story 1-bay steel frame (**Fig.6**) in case of M_1/M_2=1. The load pattern vector used in the pushover limit analysis and the reference points obtained on the yield surface are shown in **Fig.9**.

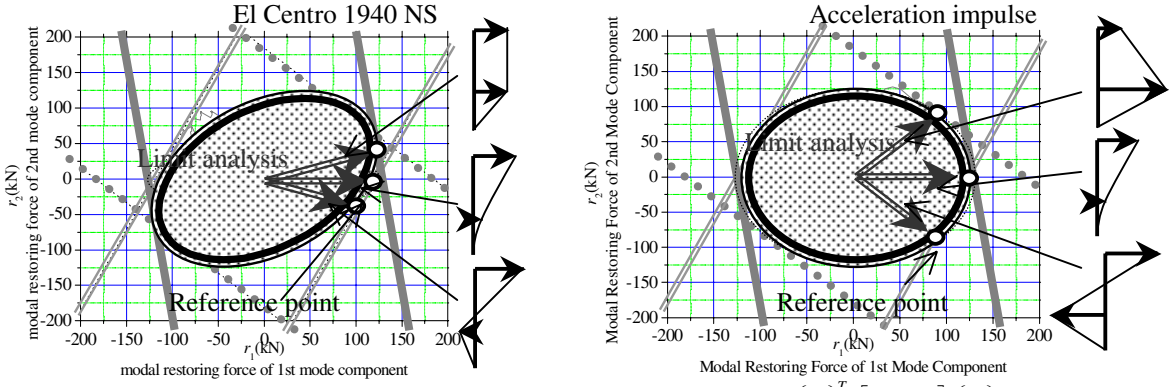

Yield ellipse $\begin{Bmatrix}{}_1r\\{}_2r\end{Bmatrix}^T\cdot\begin{bmatrix}6.5 & -1.1\\ -1.1 & 9.5\end{bmatrix}\cdot\begin{Bmatrix}{}_1r\\{}_2r\end{Bmatrix}=10^5$

Yield ellipse $\begin{Bmatrix}{}_1r\\{}_2r\end{Bmatrix}^T\cdot\begin{bmatrix}6.5 & 0\\ 0 & 6.4\end{bmatrix}\cdot\begin{Bmatrix}{}_1r\\{}_2r\end{Bmatrix}=10^5$

Fig.9 Elliptic yield surface model of 2-story 1-bay steel frame (M_1/M_2=1)

Fig.7 (b), (c) and **Fig.8 (b), (c)** show the loci of modal restoring force of the numerical response results with yield polyhedron model and elliptic yield surface model, respectively. Three loci for the test and the two analyses look very similar basically, and this supports the validity of the yield surface models proposed.

As for the results of the impulse cases shown in **Fig.7** and **Fig.8**, the initial behavior of modal restoring force point simulated by the numerical response analysis shows a good agreement with that of pseudo-dynamic response test, especially for initial behavior immediately after the impact is given. As for the elastic free vibration loci, which follow after the point leaves the boundary of failure surface, a discrepancy between the test and the two analyses is observed.

EXAMPLE OF MIDDLE-RISE STEEL MOMENT-RESISTING FRAME

In this section, 9-story 3-bay steel moment-resisting frame is taken for the comparison and is analyzed by member-hysteresis based detailed analysis.

Member-hysteresis based detailed analysis of 9-story 3-bay frame

A 9-story 3-bay steel moment-resisting frame shown in **Fig.10** is studied hereafter. The member properties and floor weight are shown in **Table 3** and **Table 4**, respectively. A constant modal-damping ratio of 2% of critical damping is considered for all the vibration modes. The elastic vibration periods are shown in **Table 5**. The base shear coefficient is 0.266.

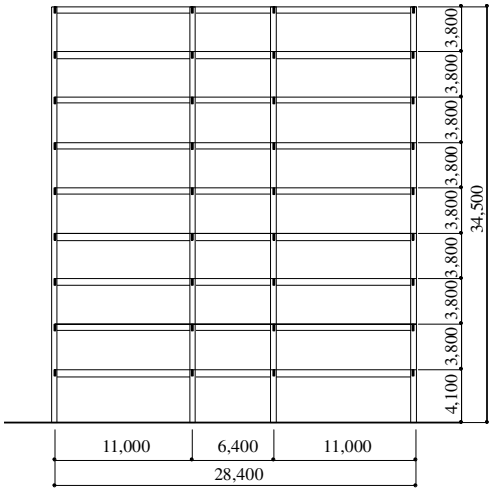

Fig.10 9-story 3-bay steel moment-resisting frame

Table 3 Member properties

(Column)

Story	Moment of inertia (cm^4)	Plastic moment capacity(kN m)
1^{st}	141,000	1,840
2^{nd}~3^{rd}	128,000	1,680
4^{th}~6^{th}	115,000	1,510
7^{th}~9^{th}	102,000	1,330

(Beam)

Story	Moment of inertia(cm^4)	Plastic moment capacity(kN m)
2^{nd}~4^{th}	59,800	713
5^{th}~6^{th}	53,800	643
7^{th}~Roof	45,700	545

Table 4 Floor weight

Story	2nd	3rd	4th	5th	6th	7th	8th	9th	Roof
Mass	0.107M	0.106M	0.106M	0.106M	0.106M	0.106M	0.106M	0.106M	0.152M

Table 5 Elastic vibration periods

Mode	1st	2nd	3rd	4th	5th	6th	7th	8th	9th
Period	1.98sec	0.65sec	0.35sec	0.22sec	0.15sec	0.11sec	0.09sec	0.07sec	0.06sec

This frame is analyzed for the ground acceleration records of El Centro 1940 NS (PGA=7.0m/sec^2), Fukiai 1995 NS (PGA=8.5m/sec^2), Hachinohe 1968 EW (PGA=4.5m/sec^2), and an acceleration impulse (initial velocity=1.0m/sec). The details of the ground motions are shown in **Table 6**. The acceleration response spectra are shown in **Fig.11**.

Table 6 Details of ground motions

Ground motion	Earthquake	Peak ground acceleration	Duration
El Centro 1940 NS	Imperial valley	7.0 m/sec^2	10sec
Hachinohe 1968 EW	Tokachi-oki	4.5 m/sec^2	20sec
Fukiai 1995 NS	Hyogoken-nanbu	8.5 m/sec^2	20sec

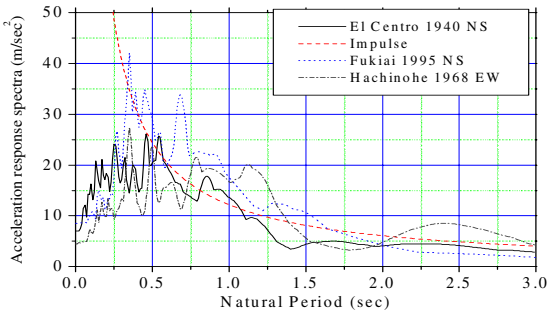

Fig.11 Acceleration response spectra (Damping=2%)

Member-hysteresis based response analysis is performed based on the ordinary plastic-hinge forming method. **Fig.12** shows the time histories of story angles at the 1st story and also at the 9th story of the frame in case of El Centro 1940 NS. **Fig.13** shows the loci of modal restoring force of 1st and 2nd mode components in case of El Centro 1940 NS. **Fig.14** shows the distribution of maximum story drift angles.

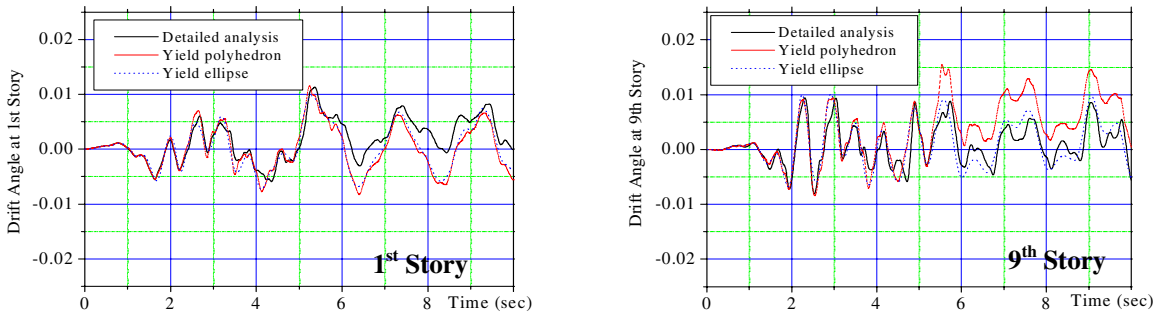

Fig.12 Time histories of story drift angles (El Centro 1940 NS)

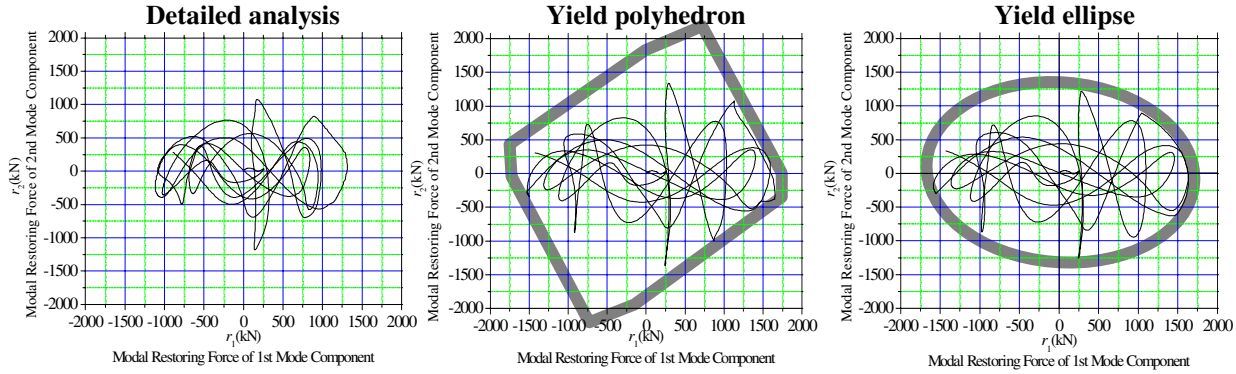

Fig.13 Loci of modal restoring force of 1st and 2nd mode components (El Centro 1940 NS)

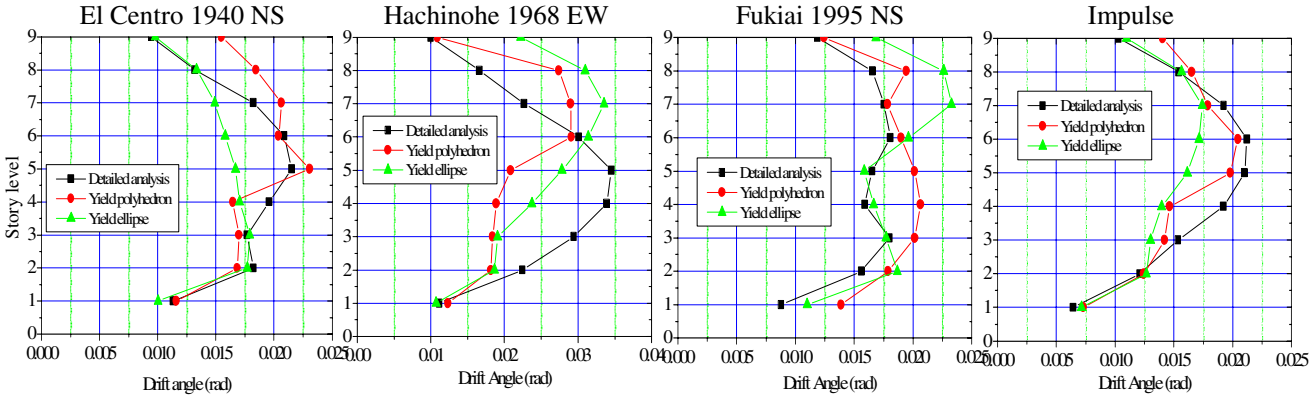

Fig.14 Distribution of maximum story drift angles

Simplified plastic failure surface models of 9-story 3-bay frame

As mentioned in the previous sections, a plastic failure surface against the plastic collapse is approximated by a simplified yield polyhedron model with a reduced number of failure modes. Relevant failure modes selected by the FOSM and PNET procedure described in the previous section, Eqs. (11) and (13), are shown in **Fig.15**. The safety domain is given as the yield polyhedron in 9-dimentional modal force space, which is bounded by the pairs of parallel hyper-planes corresponding to the failure modes as shown in **Fig.15**.

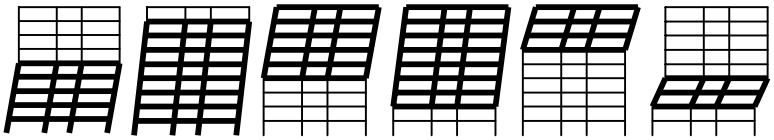

El Centro 1940 NS, Hachinohe 1968 EW

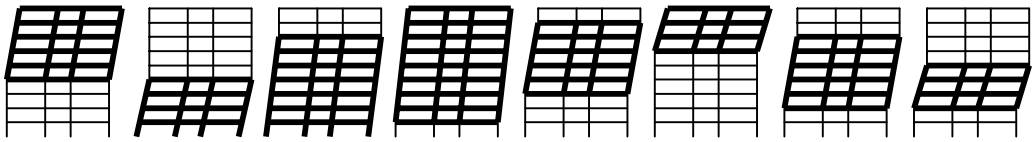

Fukiai 1968 NS

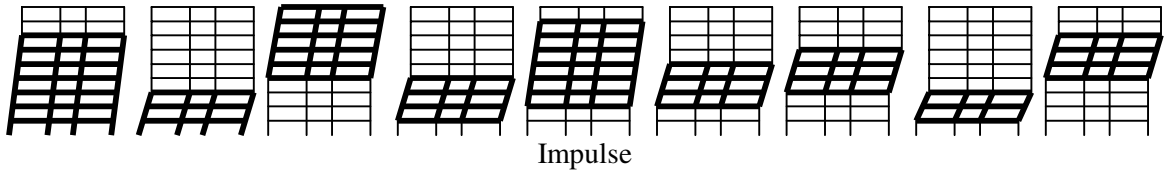

Fig.15 Relevant failure modes selected by FOSM and PNET

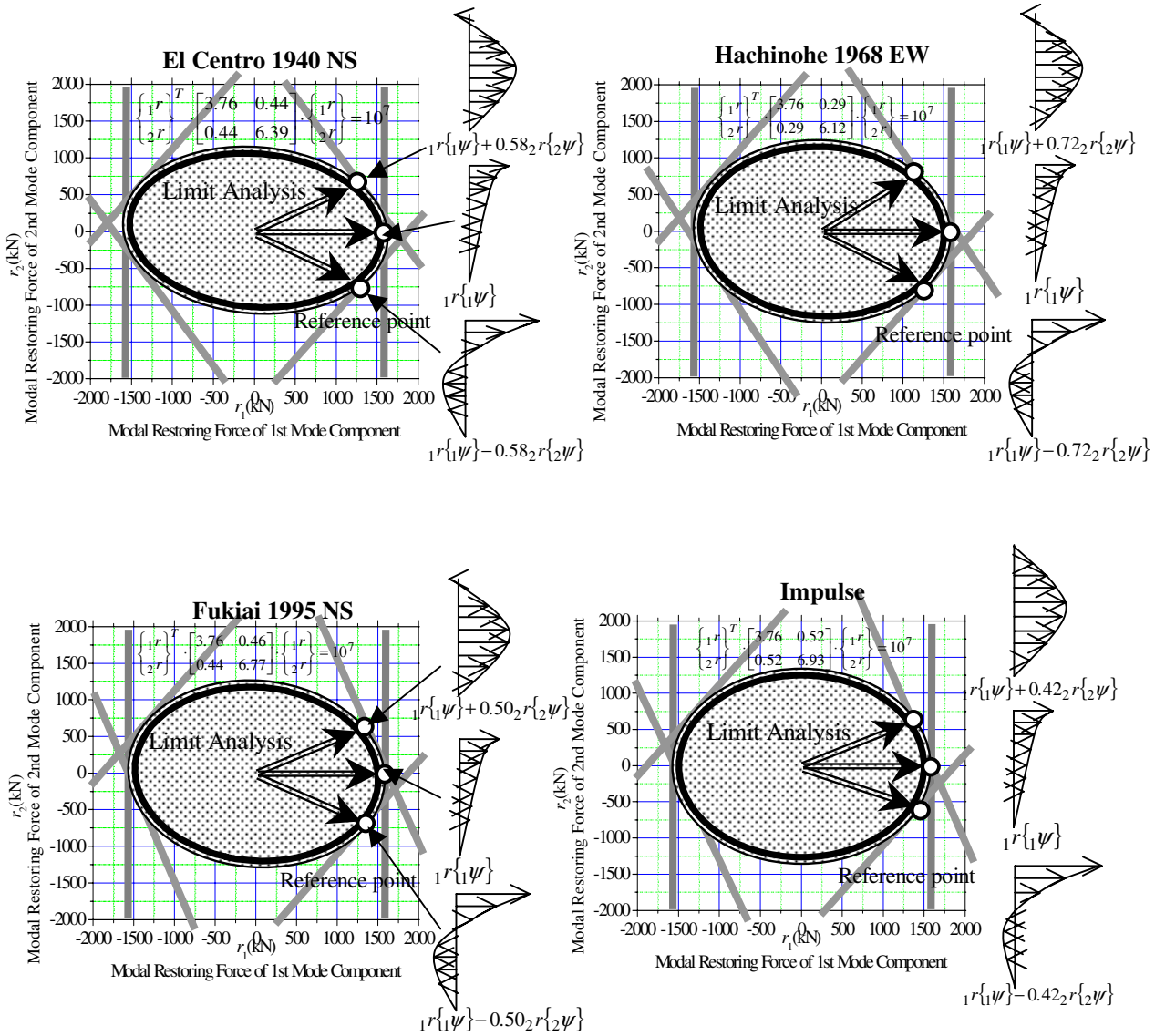

Fig.16 Yield ellipse arranged from reference points

As for the yield ellipse model in 2-dimensional modal restoring force space, the vibration modes are reduced to only two vibration modes, the 1st and the 2nd vibration modes. Pushover limit analysis is performed on the frame by using only three load patterns, the 1st mode pattern, the 1st mode plus the 2nd mode pattern, and the 1st mode minus the 2nd mode pattern. Such a pushover analysis determines three reference points or collapse states on the 1st and 2nd modal restoring force space as shown in **Fig.16**, and a yield ellipse model is arranged to include these three reference points. The yield ellipse determined is also shown in **Fig.16**.

Response analysis with simplified plastic failure surface model of 9-story 3-bay frame

The response analyses with simplified plastic surface models for the ground motions as shown in Table 6 are performed. Following two cases are studied:

1) Full vibration mode analysis with a yield polyhedron model with the relevant failure modes as shown in **Fig.15**
2) Partial vibration mode analysis with a yield ellipse model (2-degree-of-freedom, one element or one elliptic function checked)

These two cased are compared with the member-hysteresis based detailed analysis (9-degree-of-freedom, 63 elements, 126 plastic hinges checked).

The result of time history of story drift angle in case of El Centro 1940 NS is shown in **Fig.12**. The result of loci of modal restoring force in case of El Centro 1940 NS is shown in **Fig.13**. The results of distribution of maximum story drift angle are shown in **Fig.14**.

The maxima of story drift angle in 2) are slightly larger than case 1) and the detailed analysis. The case 1) yield polyhedron analysis seems to provide a sufficiently good prediction for practical purpose. Even the partial mode response analysis with a yield ellipse approximation provides an acceptable result, and it can trace the member-hysteresis based detailed analysis in outline.

CONCLUDING REMARKS

A simplified method of non-linear dynamic response analysis on a steel moment-resisting frame to a seismic action is proposed in this paper. The method is based on the two kinds of models for a safety domain against plastic collapse or a global yield surface of a frame. One is a yield polyhedron model with reduced number of failure modes by the first-order second-moment reliability method, and the other is a hyper-ellipsoidal model arranged to share some exact reference points on the yield surface obtained from pushover limit analysis. The validity of these two models are checked by comparison with member-hysteresis based detailed analysis of 9-story 3-bay frame and a pseudo-dynamic response test on a 2-story 1-bay steel moment-resisting frame specimen as well, and they are commonly found to provide consistently good predictions of global inelastic responses.

REFERENCES

1. FEMA, NEHRP Guidelines for the seismic rehabilitation of buildings, FEMA-273, Federal Emergency Management Agency, USA, 1997
2. Japanese Government, Building Standard Law of Japan revised, 1998
3. Khandelwal P., Ohi K. and Fang P., “A Simple Proposal for Ultimate Seismic Demand Evaluation of Moment Resisting Steel Frames,” Journal of structure and Construction Engineering, Architectural Institute of Japan, Vol.545, pp.141-149, 2001 (in Japanese)
4. Davenport, A.G., “Note on the Distribution of the Largest Value of a Random Function with Application to Gust Loading,” Proceedings of the Institution of Civil Engineering, Vol.28, pp.187-196, 1964
5. Shibata A., New Earthquake Resistant Structural Analysis, Morikita Press Co. Ltd., pp.188-191, 1993 (in Japanese)
6. Ang, A.H.S. and Tang, W.H., Probability Concepts in Engineering Planning and Design Volume 2 Decision, Risk and Reliability, John Wiley & Sons, pp.504-506, 1984